JOURNAL OF MAGNETIC RESONANCE **134,** 189–193 (1998)
ARTICLE NO. MN981479

The New Active-Coupling-Pattern Tilting Experiment for an Efficient and Accurate Determination of Homonuclear Coupling Constants

Wiktor Koźmiński

Department of Chemistry, Warsaw University, ul. Pasteura 1, 02-093 Warsaw, Poland

Received December 16, 1997; revised April 7, 1998

A new constant-time COSY experiment which allows an efficient determination of accurate homonuclear coupling constant values is presented. Characteristic features include an improved scheme for homonuclear *a*ctive-*c*oupling-pattern *t*ilting (ACT) and an *a*rbitrarily *s*caled *s*hift and *c*oupling *i*nformation (ASSCI) design of the F_1 domain. As a result, simple and easy to interpret tilted cross-peak patterns, even for two-spin systems, are obtained with good sensitivity. The relative spacing of chemical-shift differences and coupling splittings is largely under experimental control. The effectiveness of the spectral region selective variant of the new sequence is demonstrated by a determination of the $^3J_{HN,H\alpha}$ couplings in a peptide sample. The multiplet-selective variant is shown to produce good results with a terpene. The superiority of the new ACT scheme is additionally demonstrated by an ACT–*J* spectrum of the peptide. © 1998 Academic Press

Key Words: **COSY; constant-time; J-couplings; active-coupling-pattern tilting; Accordion spectroscopy.**

Previously, we proposed an active-coupling-pattern tilting procedure for efficient determination and assignment of (i) heteronuclear coupling constants from heteronuclear correlations (HECADE) (*1*) and of (ii) homo- and heteronuclear coupling constants from pure-phase ACT–*J* spectra (*2*). Whereas both heteronuclear applications were successful, the homonuclear ACT–*J* experiment presented did not immediately yield an assignment of the coupling constants, and the effectiveness of ACT for the simplification of the cross-peak patterns was not quite satisfying. In this Communication, a better approach for homonuclear ACT and the solution of the assignment problem by incorporating it into a ct-COSY experiment is introduced. In contrast to E.COSY (*3*) and P.E.COSY (*4*) methods, which require at least three mutually coupled spins, ACT offers the advantage of tilted peak patterns also for two-spin systems. The performance of the new method is exemplified by measuring peptide $^3J_{HN,H\alpha}$ coupling constants of a natural abundance sample in a 9/1 H_2O/D_2O solution. The established methods for determination of these important couplings use evaluation of extrema separations in absorptive and dispersive signals from phase-sensitive COSY spectra (*5*) or fitting in- and antiphase signals acquired in different experiments (*6*). In the case of isotopically enriched samples, HNCA–E.COSY and J_{HH}–TOCSY experiments (*7*) could be employed, resulting in an E.COSY cross-peak structure. Recently, another method, using spin-state *s*elective *e*xcitation (S^3E), for $^nJ_{HH}$ determination was introduced (*8*). However, it is also designed for isotopically labeled samples.

Figure 1 displays the pulse sequence scheme for the new experiment, exploiting two characteristic periods. In the first constant-time period, the chemical-shift t_1 modulation of all protons occurs and all homonuclear couplings evolve during the entire 2Δ delay. Only antiphase coherences are transferred through the subsequent double-quantum (DQ) filter. The transfer amplitude is proportional to

$$\sin(\pi J_{act} 2\Delta)\Pi \cos(\pi J_{pas} 2\Delta), \qquad [1]$$

where J_{act} and J_{pas} represent active and passive couplings, respectively. The constant-time ^1H chemical-shift evolution approach results in a significant simplification of cross-peak patterns but it limits the possible number of t_1 increments and, consequently, the maximum value of t_1. The DQ filter is optional and rejects half of the observed nondiagonal signal intensity, but it was found useful in obtaining cleaner spectra. In the second time period of t_1^* only homonuclear couplings evolve and chemical-shift evolution is refocused. The t_1^* and t_1 times are incremented synchronously, according to the Accordion spectroscopy principle (*9, 10*), creating a frequency domain encoding *a*rbitrarily *s*caled *s*hift and *c*oupling *i*nformation (ASSCI) (*1*). The number of t_1^*/t_1 increments and their ratio should be optimized considering T_2 relaxation times and the necessary resolution of both chemical-shift resolution and coupling splittings in the F_1 dimension. The last element of the pulse sequence acts either as a zero or as a selective refocusing pulse. It consists of the DPFGSE (*11, 12*) element which selects a region of interest and refocuses all interactions, and the central selective zero or π-pulse. Contrary to our previous homonuclear ACT implementation (*2*), where the central π-pulse inverted magnetization of the coupling partner, here, all selective pulses are applied to the same spins of interest. Consequently, the method can be applied to every group of spins not mutually coupled that could be selectively refocused.

1090-7807/98 $25.00

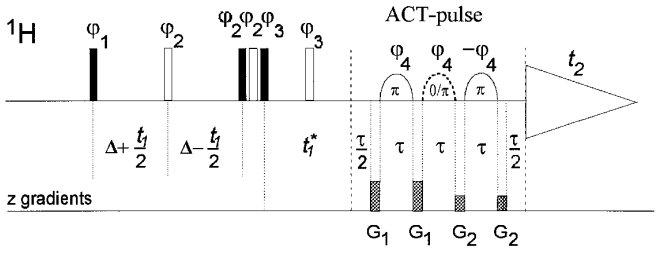

FIG. 1. Pulse sequence for ACT–ct-COSY experiment. Dark-filled and open bars represent $\pi/2$- and π-pulses, respectively. The delay 2Δ should be optimized for maximum excitation of DQ-coherences and long enough t_1 evolution. The duration of selective π-pulses is symbolized by τ. The middle, dashed selective π-pulse is applied for one of two data sets. The additional central π-pulse in the DQ filter refocuses evolution of DQ coherences during pulses and is optional. The rectangular z-gradient pulses with amplitudes of 10 and 3.8 G/cm for G_1 and G_2, respectively, were used in this work. Gradient pulse duration was set to 1 ms and followed by a 100 μs recovery delay. The RF offset should be set to the center of the F_1 dimension (H_2O resonance for samples in water) for the first three pulses, and then switched to the center of the selectively refocused region. The ACT–J experiment can be created by use of a single $\pi/2$-pulse with phase $\varphi 3$ before the t_1^* evolution period. The suggested phase cycling scheme is summarized in Tables 1 and 2.

Regardless of the t_1 modulation and the transfer amplitude and assuming that selective pulses are applied for the spin I_1, the relevant components of the density matrix for the cross-peaks of interest at point $t_2=0$ can be described by the following Cartesian product-operator terms.

For a two-spin system,

$$2I_{1x}I_{2z}\cos(\pi J_{1,2}t_1^*) + I_{1y}\sin(\pi J_{1,2}t_1^*). \qquad [2]$$

In the presence of the third coupled spin two nondiagonal signals are observed:

Cross-peak I_1–I_2	Cross-peak I_1–I_3
$2I_{1x}I_{2z}\cos(\pi J_{1,2}t_1^*)\cos(\pi J_{1,3}t_1^*)$	$2I_{1x}I_{3z}\cos(\pi J_{1,3}t_1^*)\cos(\pi J_{1,2}t_1^*)$
$-2I_{1x}I_{3z}\sin(\pi J_{1,2}t_1^*)\sin(\pi J_{1,3}t_1^*)$	$-2I_{1x}I_{3z}\sin(\pi J_{1,3}t_1^*)\sin(\pi J_{1,2}t_1^*)$
$+I_{1y}\sin(\pi J_{1,2}t_1^*)\cos(\pi J_{1,3}t_1^*)$	$+I_{1y}\sin(\pi J_{1,3}t_1^*)\cos(\pi J_{1,2}t_1^*)$
$+4I_{1y}I_{2z}I_{3z}\cos(\pi J_{1,2}t_1^*)\sin(\pi J_{1,3}t_1^*)$	$+4I_{1y}I_{2z}I_{3z}\cos(\pi J_{1,3}t_1^*)\sin(\pi J_{1,2}t_1^*)$

[3]

In the case of a sequence involving a DQ filter the I_1–I_1 diagonal peaks could be described by a sum of terms presented above, with weighting factors dependent on transfer amplitude (Eq. [1]). A subsequent selective π-pulse with the phase along the x-axis, applied for one of two data sets, inverts the signs of all terms with odd numbers of $\sin(\pi Jt_1^*)$ factors, independently of the number of spins coupled to I_1. Hence, proper coaddition of terms which differ in phase by $\pi/2$ in both time domains is possible, and in contrast to the usual homonuclear J-resolved experiments pure absorption spectra could be obtained. The experiment presented can easily be turned into a J-resolved variant, (ACT–J), by omission of the first constant-time period and simply starting the sequence with a $\pi/2$-pulse just prior to the t_1^* evolution. In this case, only one signal, described by

$$\begin{aligned} &I_{1y}\cos(\pi J_{1,2}t_1^*)\cos(\pi J_{1,3}t_1^*) \\ &-2I_{1x}I_{2z}\sin(\pi J_{1,2}t_1^*)\cos(\pi J_{1,3}t_1^*) \\ &-2I_{1x}I_{3z}\cos(\pi J_{1,2}t_1^*)\sin(\pi J_{1,3}t_1^*) \\ &-4I_{1y}I_{2z}I_{3z}\sin(\pi J_{1,2}t_1^*)\sin(\pi J_{1,3}t_1^*) \end{aligned} \qquad [4]$$

would be observed and the selective π-pulse along the x-axis changes the signs of terms with odd numbers of $\cos(\pi Jt_1^*)$ factors.

As pointed out in an earlier communication (*2*) the same signal-to-noise ratio as that in previous implementations can be achieved with only half the number of scans by measuring two data sets with the ACT-pulse set to 0 and to π, respectively. In the case of ACT–J experiments, the data should be processed directly according to the echo–antiecho method (*13*, *14*). In HECADE experiments (*1*) the gradient echo- and antiecho selection should be changed with the ACT-pulse angle and processed in the usual way. In the case of an ACT–ct-COSY sequence, the States–TPPI (*15*) method of t_1 interferogram construction is to be preferred. Two echo- and antiecho-like data sets are generated, and processed accordingly. The first data set consists of the sum of orthogonal shift-evolution terms and the second one of their difference with additional sign inversion of all terms with odd numbers of $\sin(\pi Jt_1^*)$ factors.

For a two-spin system four different terms for the echo- and antiecho data set are observed:

$$\begin{aligned} \text{echo} = {} & 2I_{1x}I_{2z}\cos(\pi J_{1,2}t_1^*)\cos(\omega_I t_1) \\ & + I_{1y}\sin(\pi J_{1,2}t_1^*)\cos(\omega_I t_1) \\ & + 2I_{1y}I_{2z}\cos(\pi J_{1,2}t_1^*)\sin(\omega_I t_1) \\ & - I_{1x}\sin(\pi J_{1,2}t_1^*)\sin(\omega_I t_1) \\ \text{antiecho} = {} & 2I_{1x}I_{2z}\cos(\pi J_{1,2}t_1^*)\cos(\omega_I t_1) \\ & - I_{1y}\sin(\pi J_{1,2}t_1^*)\cos(\omega_I t_1) \\ & - 2I_{1y}I_{2z}\cos(\pi J_{1,2}t_1^*)\sin(\omega_I t_1) \\ & - I_{1x}\sin(\pi J_{1,2}t_1^*)\sin(\omega_I t_1). \end{aligned} \qquad [5]$$

The data should be processed by calculation of the sum and difference of echo- and antiecho data, and two new data sets are obtained:

$$\begin{aligned} \text{echo} + \text{antiecho} = {} & 4I_{1x}I_{2z}\cos(\pi J_{1,2}t_1^*)\cos(\omega_I t_1) \\ & - 2I_{1x}\sin(\pi J_{1,2}t_1^*)\sin(\omega_I t_1) \\ \text{echo} - \text{antiecho} = {} & 4I_{1y}I_{2z}\cos(\pi J_{1,2}t_1^*)\sin(\omega_I t_1) \\ & + 2I_{1y}\sin(\pi J_{1,2}t_1^*)\cos(\omega_I t_1) \end{aligned} \qquad [6]$$

After $\pi/2$ phase correction of the second data set, the genera-

TABLE 1
Phase Cycling for ACT–ct-COSY Experiment Depicted in Fig. 1

	Data set #1		Data set #2
φ_1	$8(x, y), 8(y, -x), 8(-x, -y), 8(-y, x)$		$8(x, -y), 8(y, x), 8(-x, y), 8(-y, -x)$
φ_2		$16x, 16y, 16-x, 16-y$	
φ_3		$x, x, y, y, -x, -x, -y, -y,$	
φ_4		$8x, 8y$	
ACT-pulse	0		π
$\varphi_{receiver}$	$2(x, y, -y, x, -x, -y, y, -x),$ $2(-x, -y, y, -x, x, y, -y, x)$		$x, y, y, -x, -x, -y, -y, x,$ $2(-x, -y, -y, x, x, y, y, -x,),$ $x, y, y, -x, -x, -y, -y, x,$

Note. The two data sets are stored in separated memory locations, and should be combined as for echo–antiecho experiments; the sign of the tilting could be changed by exchange of the ACT-pulse angle and the receiver phases between two data sets.

tion of pure-phase spectra by the method of States *et al.* (*16*) is possible, which results in coaddition of in- and antiphase terms. For the even t_1^*/t_1 increments, the phase of the first pulse and receiver is reversed to shift axial peaks to the edge of the spectra. The appropriate phase cycling schemes for ACT–ct-COSY and homonuclear ACT–*J* experiments are summarized in Tables 1 and 2, respectively.

The theoretical sensitivity of the proposed method could be compared with a DQF–COSY experiment. There are two differences: (i) For the same homonuclear coupling evolution time ACT–ct-COSY sequence is longer by constant-time period and ACT-pulse, which could reduce sensitivity due to T_2 relaxation, and (ii) transfer amplitude, described in Eq. [3], in the proposed experiment is constant but strongly dependent on constant-time evolution duration (2Δ). For DQF–COSY this amplitude depends on t_1-evolution time and is averaged. Hence, sensitivity of ACT–ct-COSY could be higher in the case where the Eq. [3] condition is perfectly matched and lower when 2Δ is far from the optimum. The F_2 selectivity of the ACT–ct-COSY experiment allows easily for long t_2 and consequently good resolution. Additionally, in comparison to other COSY variants, due to simplified multiplet patterns the spectra are less susceptible to signal overlapping. Due to evolution of the same coherences in t_1^* and t_2 periods, application of the proposed method is limited to the case where the homogeneous linewidth is smaller than the coupling magnitude. In the opposite case E.COSY-type methods requiring three spin systems, with separation of relevant cross-peak components larger in the F_1 than in the F_2 domain, should be preferred. However, in the case of inhomogeneous line broadening, the ACT–ct-COSY method is expected to be favorable due to increased resolution in the F_1 domain.

As an example, Fig. 2 displays a contour plot of an NH region-selective ACT–ct-COSY spectrum displaying all vicinal $^3J_{HN,\,H\alpha}$ coupling constants of the major isomer in a 25 m*M*

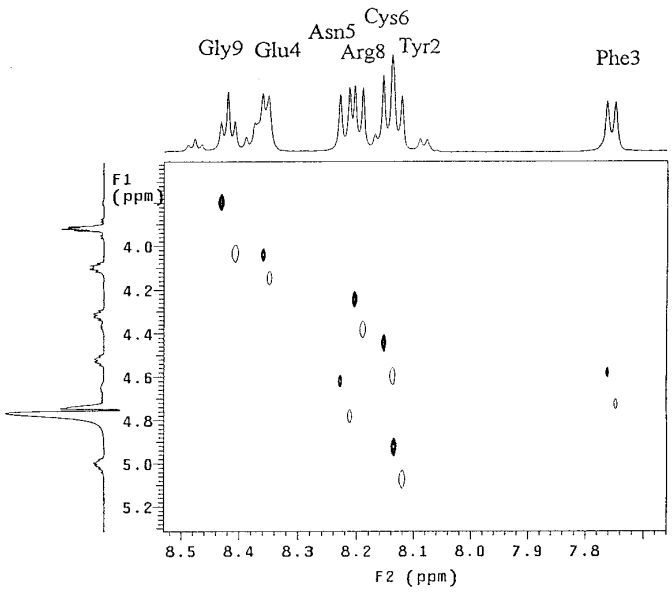

FIG. 2. Expanded HN–Hα region from the analog of the [Me, Ala^7]AVP–vasopressin spectrum obtained by an ACT–ct-COSY sequence. Contour levels for the major isomer only are shown. For negative peaks only one level was plotted. All cross-peaks display tilted active homonuclear coupling in antiphase in both dimensions. The spectrum was acquired from a 25 m*M* 90% H_2O/D_2O solution. Eight scans were coherently added for each data set for 160 t_1/t_1^* increments. The maximum t_1 and t_1^* times were 32.6 and 326 ms, respectively. Eight hundred complex points to the maximum t_2 time of 0.8 s was acquired. Water signal presaturation, with the $\gamma B_1/2\pi$ of ca. 40 Hz, during the relaxation delay of 1.4 s was used. The delay 2Δ of 40 ms was used. A 10.9 ms RE–BURP amplitude modulation profile (*15*) was employed for selective refocusing. The data matrix was zero-filled to 2048 × 4096 complex points, and no weighting functions prior to Fourier transformation were applied.

TABLE 2
Basic Phase Cycling for Homonuclear ACT–*J* Experiment

	Data set #1	Data set #2
φ_3	$x, x, y, y, -x, -x, -y, -y$	
φ_4	x, y	
ACT-pulse	0	π
$\varphi_{receiver}$	$x, x, y, y, -x, -x, -y, -y$	$x, -x, -y, y, -x, x, y, -y,$

Note. The two data sets should be processed as for ACT–ct-COSY.

TABLE 3

Coupling Constants $^3J_{NH,H\alpha}$, Obtained from ACT–ct-COSY Experiment, of the Major Isomer of the [Me, Ala^7]AVP–Vasopressin Analog

	Tyr^2	Phe^3	Glu^4	Asn^5	Cys^6	Arg^8	Gly^9
$^3J_{HN,\,H\alpha}$ (Hz)	7.4	7.3	5.3	8.1	7.7	7.0	6.0[a]

Note. Couplings were read from F_2 projections. The accuracy is estimated to be ca. 0.1 Hz.

[a] For Gly^9 the two $^3J_{HN,\,H\alpha}$ coupling constants with Hα protons are equal within limits of error.

solution of the [Me, Ala^7]AVP–vasopressin analog in 9/1 H_2O/D_2O. The solution contains two isomers in approximate 4:1 ratio. Table 3 summarizes the absolute values of coupling constants obtained in this experiment. The magnitude of $^3J_{HN,\,H\alpha}$ coupling constants obtained from F_2 and F_1 projections is the same within error limits. Note that the HN–H$_\alpha$ correlations at F_1 frequencies near the water resonance are clearly visible. Figure 3 shows a homonuclear ACT–*J* spectrum of the same sample. In both cases, due to the improved homonuclear ACT approach, no disturbing contribution of the complementary tilted pattern is observed, as in a previously reported ACT–J experiment (*2*).

The multiplet-selective version of the ACT–ct-COSY experiment has been applied to an H(1) proton of (–)-menthol in $CDCl_3$. The resulting spectrum is shown in Fig. 4. The active coupling is always in antiphase, allowing the assignment of all

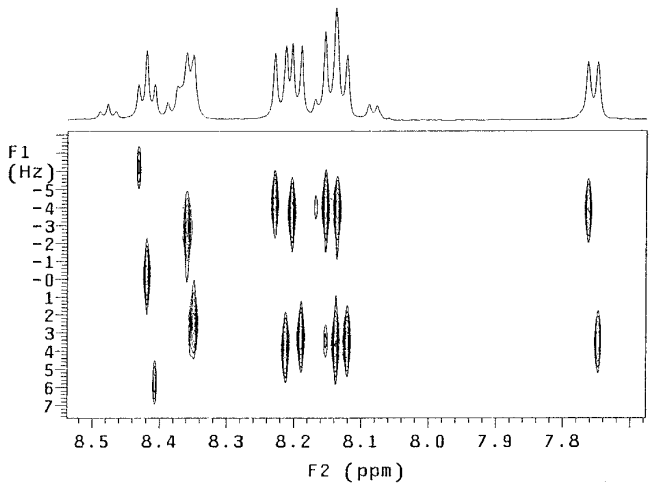

FIG. 3. Part of contour plot of the ACT–J spectrum of the [Me, Ala^7]AVP–vasopressin analog sample. Signals of the dominant isomer only are shown. In contrast to the ACT–ct-COSY spectrum all couplings are in phase in both dimensions. A 10.9 ms RE–BURP amplitude modulation profile (*15*) was employed for selective refocusing. Two data sets were acquired with eight scans for each of 16 t_1^* increments. The maximum t_1^* and t_2 times were set to 0.5 and 1.0 s, respectively. The data matrix, containing 16 × 1000 complex points, in t_1^* and t_2, respectively, was zero-filled to 64 × 2048 complex points. No weighting functions prior to Fourier transformation were applied. Water signal presaturation, with a $\gamma B_1/2\pi$ of ca. 40 Hz, during the relaxation delay of 1.4 s was used.

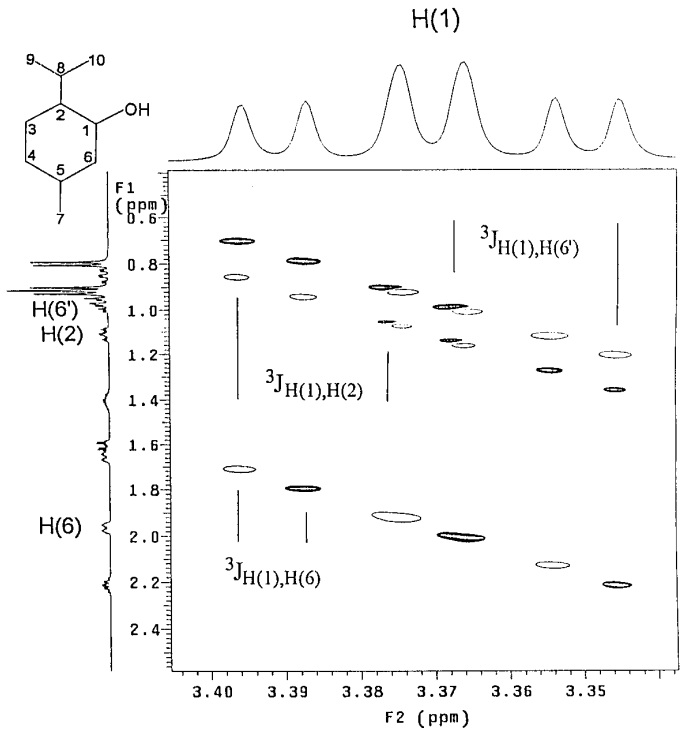

FIG. 4. Expansion of the ACT–ct-COSY spectrum of a 0.5 *M* (–)-menthol sample in $CDCl_3$. The active couplings are in antiphase and the passive ones in phase in both dimensions. The tilted cross-peak pattern helps in analysis and assignment of couplings. Eight scans were coherently added for each data set for 128 t_1/t_1^* increments. The maximum t_1 and t_1^* times were 66.4 and 664 ms, respectively. The maximum t_2 time was set to 1.4 s (256 complex points). The delay 2Δ was set to the maximum value of t_1. A 48.6 ms RE–BURP amplitude modulation profile (*15*) was employed for selective refocusing of the H(1) proton. A relaxation delay of 1 s was used. The data matrix was zero-filled to 512 × 1024 complex points, and no weighting functions prior to Fourier transformation were applied.

observed coupling constants. The vicinal coupling constants of H(1) with H(6′) and H(2) are very similar.

All the spectra presented were acquired at 300 K on a Varian Unity Plus 500 spectrometer, equipped with a Performa I z-PFG unit, and using a standard 5 mm ID_PFG probehead. For selective refocusing the RE–BURP (*17*) amplitude modulation profile was used in all cases. Hard ^{1}H $\pi/2$ pulses of 12 μs were used.

In conclusion, the new sequence presented permits an accurate and relatively sensitive determination of homonuclear coupling constants. Tilted cross-peak patterns are obtained for all spin systems; however, this tilt does not contain information about the relative signs of the coupling constants. The ACT–*J* part of the proposed sequence, with t_1^* evolution, could be combined with other known 2D NMR methods with different t_1 evolution periods. The proposed ACT–ct-COSY method seems to be particularly useful for the two spin systems such as HN–H$_\alpha$ systems in peptides at natural isotope abundances. However, it can also be applied to the analysis of complicated multiplet patterns in a variety of organic compounds.

ACKNOWLEDGMENTS

The work was supported by the KBN as the 12-501/03/BST-562/33/97 project. The author thanks D. Nanz for valuable comments and suggestions, and I. Zhukow and J. Wójcik, of the Institute of Biochemistry and Biophysics, Polish Academy of Sciences, and J. Ciarkowski, Z. Grzonka, and F. Kasprzykowski, of the Department of Chemistry, Gdańsk University, for the loan of the [Me, Ala^7]AVP–vasopressin analog sample and ^{1}H NMR signal assignments.

REFERENCES

1. W. Koźmiński and D. Nanz, *J. Magn. Reson.* **124,** 383 (1997).
2. W. Koźmiński, S. Bienz, S. Bratovanow, and D. Nanz, *J. Magn. Reson.* **125,** 193 (1997).
3. C. Griesinger, O. W. Sorensen, and R. R. Ernst, *J. Am. Chem. Soc.* **107,** 6394 (1985).
4. L. Mueller, *J. Magn. Reson.* **72,** 383 (1987).
5. Y. Kim and J. H. Prestegard, *J. Magn. Reson.* **84,** 9 (1989).
6. J. J. Titman and J. Keeler, *J. Magn. Reson.* **89,** 640 (1990).
7. C. Griesinger, H. Schwalbe, J. Schleucher, and M. Sattler, *in* "Two Dimensional NMR Spectroscopy: Applications for Chemists and Biochemists" (W. R. Croasmun and R. M. K. Carlson, Eds.), 2nd ed., p. 568, VCH Publishers, New York (1994).
8. A. Meissner, J. O. Duns, and O. W. Sorensen, *J. Magn. Reson.* **128,** 92 (1997).
9. G. Bodenhausen and R. R. Ernst, *J. Magn. Reson.* **45,** 367 (1981).
10. G. Bodenhausen and R. R. Ernst, *J. Am. Chem. Soc.* **104,** 1304 (1982).
11. T. L. Hwang and A. J. Shaka, *J. Magn. Reson.* A **112,** 275 (1995).
12. K. Stott, J. Keeler, Q. N. Van, and A. J. Shaka, *J. Magn. Reson.* **125,** 302 (1997).
13. J. Boyd, N. Soffe, B. John, D. Plant, and R. Hurd, *J. Magn. Reson.* **98,** 660 (1992).
14. J. R. Tolman, J. Chung, and J. H. Prestegard, *J. Magn. Reson.* **98,** 462 (1992).
15. D. J. Marion, M. Ikura, R. Tschudin, and A. Bax, *J. Magn. Reson.* **85,** 393 (1989).
16. D. J. States, R. A. Haberkorn, and D. J. Ruben, *J. Magn. Reson.* **48,** 286 (1982).
17. H. Geen and R. Freeman, *J. Magn. Reson.* **93,** 93 (1991).